fire

Article

The Effects of Solvent Extraction on the Functional Group Structure of Long-Flame Coal

Jun Guo [1,2], Yanping Quan [1,*], Hu Wen [1,2], Xuezhao Zheng [1,2], Guobin Cai [1,2] and Yan Jin [1,3]

[1] College of Safety Science and Engineering, Xi'an University of Science and Technology, Xi'an 710054, China; guojun@xust.edu.cn (J.G.); wenhu@xust.edu.cn (H.W.); zhengxuezhao@xust.edu.cn (X.Z.); 19220214086@stu.xust.edu.cn (G.C.); 15258821069@163.com (Y.J.)
[2] Key Laboratory of Western Mine and Hazard Prevention, Ministry of Education of China, Xi'an 710054, China
[3] Sinopec Sales Co., Ltd. Taizhou Petroleum Branch, Taizhou 318000, China
* Correspondence: 21220226136@stu.xust.edu.cn

Abstract: The functional group structures of coal molecules are one of the most important factors affecting spontaneous combustion. However, it is difficult to determine the exact effects of such structures. Extraction technology is able to modify the functional groups in coal as a means of inhibiting spontaneous combustion reactions. The present work extracted coal from the Caojiatan mine in northern Shaanxi, China, with various solvents. The extraction effectiveness of these solvents was found to decrease in the order of dioctyl sulfosuccinate (AOT) > water > n-hexane > cyclohexane + AOT + ethanol > cyclohexane > ethanol > methanol. With the exception of the AOT, the concentration of functional groups in the extracted coal was decreased compared with that in a control specimen extracted using only water. Ethanol, n-hexane, and methanol provided the optimal extraction efficiencies in terms of capturing coal molecules with aromatic structures, aliphatic structures, and oxygen-containing groups, respectively. The results of this work are expected to assist in future research concerning the extraction of coal molecules with specific functional groups. This work also suggests new approaches to the active prevention and control of spontaneous combustion during the mining, storage, and transportation of coal.

Keywords: coal spontaneous combustion; targeted extraction; functional groups

check for updates

Citation: Guo, J.; Quan, Y.; Wen, H.; Zheng, X.; Cai, G.; Jin, Y. The Effects of Solvent Extraction on the Functional Group Structure of Long-Flame Coal. *Fire* **2023**, *6*, 307. https://doi.org/10.3390/fire6080307

Academic Editors: Wei Liu, Caiping Wang, Bobo Shi and Zeyang Song

Received: 20 July 2023
Revised: 4 August 2023
Accepted: 8 August 2023
Published: 10 August 2023

1. Introduction

Coal mining efficiency has been greatly improved by the adoption of retreating subsidence, high-rise grouting, and longwall mining together with other technologies. However, these techniques have also led to increasingly complex and harsh underground mining environments that are associated with spontaneous combustion and frequent underground fires [1–4]. Unfortunately, at present, the prediction and analysis of such incidents is challenging and new technologies together with in-depth theoretical research are required to identify risk factors [5,6]. Assessments of these factors would allow the effective prevention and control of coal spontaneous combustion. In particular, there is a need to study the characteristics of spontaneous combustion in coal seams.

In recent years, the rapid development of microscopic-scale analytic technologies has allowed the reaction characteristics of coal molecules to be evaluated. Such analyses are commonly based on the use of solid-liquid extraction to separate various mixtures. This separation technology is widely used in many fields, including medicine and biology, as well as in the food and chemical industries. As an example, Li et al. [7] extracted corn whiskers with both ethyl acetate and methanol to obtain DL-epiloliolide, N-p-hydroxy-cis-coumaroyltyramine, β-Sitosterul, and other compounds. Wang et al. [8] extracted extracellular proteins and alkaline phosphatase from thallus with n-butanol and used this extract to inhibit the activity of Staphylococcus aureus. Hu et al. [9] used various polar solvents (ethyl acetate and n-butanol) to extract nuclear biomass components from hawthorn and studied the antioxidant properties of these substances. Wang [10] obtained anti-aging compounds from dandelion, chicory root, and Perilla leaves using a supercritical extraction method.

The successful application of extraction in various industries suggests that this technique could also be applied to the prevention and control of coal fires. Because the molecular structure of coal is based on the condensation polymerization of benzene rings with alkyl side chains and coal also contains bridging bonds and other structures, it should be possible to use various solvents to separate coal molecules according to their physical and chemical properties [11–15]. Subsequent analyses of the microscopic coal structures could provide information concerning the spontaneous combustion mechanism. In prior work, Zhang et al. [16] used a variety of solvents, including cyclohexane and carbon disulfide, to carry out extraction trials and determined the capacities of these solvents. Zhang also employed Fourier transform infrared (FTIR) spectroscopy to determine the roles of various functional groups in the spontaneous combustion of coal. Ma et al. [17,18] extracted Hefeng (a location name) coal with petroleum ether, methanol, carbon disulfide, and acetone using a continuous five stage process involving ultrasonication together with either single or mixed solvents. The molecular structures of the extracted materials were ascertained using gas chromatography-mass spectrometry. The combination of acetone and carbon disulfide was found to promote the dissolution of coal molecules with hydroxy groups. Deng et al. [19,20] used an imidazole-based ionic liquid to extract coal specimens while degrading various functional groups. Thermogravimetric data indicated that [BMIM][BF_4] had the strongest effect, based on the reaction mechanism shown in Figure 1. Marek et al. [21] proposed that alcohols could be the most effective extraction solvents and performed trials using n-heptane, toluene, n-butanol, and three other isomeric alcohols with five Polish lignite specimens. The results showed that n-butanol provided the highest degree of extraction. The results of this work also indicated that the extraction efficiency was maximized only when the solvent was able to extract specific functional groups so as to weaken the spontaneous combustion of the extracted coal sample.

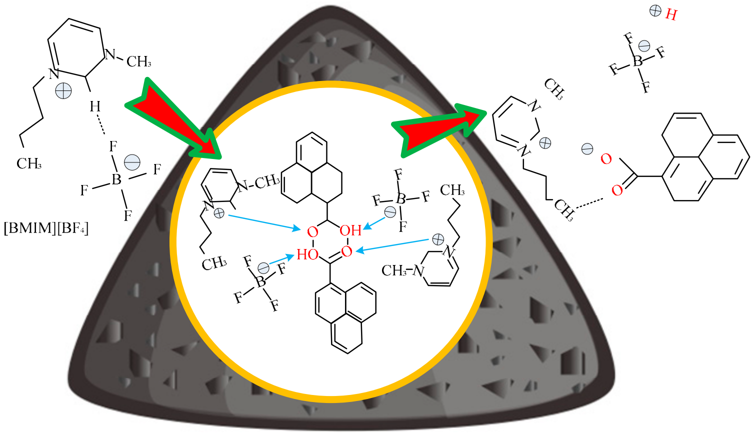

Figure 1. Diagram of the reaction between an ionic liquid and functional groups in coal molecules. (Figure source: Author's own work).

Based on this prior work, it is evident that the active functional groups such as oxygen-containing functional groups and alkyl side chain groups in coal are the main causes of spontaneous combustion of coal. The bridge bonds of coal molecules can be broken through extraction technology, resulting in functional groups being stripped. Finally, the spontaneous combustion of coal will be weakened. However, the effects of this extraction process under specific conditions require further study [22,23]. In the present work, the effects of different extraction solvents on the functional group structure of coal are compared based on trials involving pure solvents and solvent mixtures. This research is expected to provide theoretical guidance for subsequent research concerning the molecular structure of coal and the effects of extraction.

2. Experimental Section

2.1. Selection of Extractants

The spontaneous combustion of coal is an extremely complex process involving the reactions of various functional group structures, with certain structures being more reactive [24]. For this reason, suitable extraction agents must be identified based on the specific groups being targeted. The main categories of coal structures comprise the following. Firstly, macromolecular aromatic structures that form the main carbon chain skeletons in coal molecules will actively participate in combustion. Secondly, aliphatic side-chains will play a key role in terms of heat generation by participating in cracking reactions with oxygen. Lastly, oxygen-containing structures, such as hydroxy or phenolic groups, may also undergo reactions. During combustion, oxygen adsorption reactions generate energy and so intensify the initial combustion reaction. Coal is made of condensed ring polymers primarily comprising aromatic and nonaromatic moieties connected through bridging bonds [25]. The solvent extraction of coal is intended to remove active groups such as these by degrading the connecting structures, such that spontaneous combustion reactions are unlikely to occur. Table 1 summarizes a number of functional groups found in coal molecules along with suitable extractants for such groups.

Table 1. Extractants for coal and their operational principles [26–31].

The Name of the Reagent	For the Group Structure	Action Principle
carbon disulfide	associated structures (e.g., macromolecular aromatic hydrocarbons)	It affects charge transfer and breaks hydrogen bonds
cyclohexane	–C–O–C–, –OH and aliphatic hydrocarbon	Sabotaging the association between molecules
N, N-dimethyl acetamide	aliphatic hydrocarbon radical	High polarization; it has both electron donors and acceptors
acetone	aliphatic hydrocarbon–CH_3, –C–O–C–, –CH_3, –CH_2 and heteroatomic compounds	Like dissolves like
ethanol	structure of aliphatic hydrocarbons	Dissolve part of aliphatic structure or high polarity side chain group unit
ethylenediamine	–NH_2, –CH_2, –OH and other hydrogen bonds contain structures	It has a strong ability to supply electrons and break hydrogen bonds
methanol	aliphatic side chains and highly polar groups	It has strong solubility for polar compounds
petroleum ether	aliphatic hydrocarbons, aromatic hydrocarbons and heteroatomic compounds	Alkyl substitution reaction
n-hexane	hydrogen bonds with polar molecules	Absorption of organic matter
ionic liquid	different functional groups can be extracted by simple preparation and modification of ionic structures	Destruction of hydrogen bonds, branched carbonyl groups and other structures; Reduce or disperse oxygen-containing functional groups
reverse micelles	polar structures such as proteins	Reverse micellar nanoaggregates are formed by directional arrangement of hydrophilic or hydrophobic structures to control group flow

In theory, methanol will undergo alcoholysis reactions with coal molecules under relatively mild conditions [32]. The associated rupture of ester, hydrogen, or oxygen-containing bridging bonds by hydrogen supplied from the methanol will disrupt the linkages between aromatic rings in the coal macromolecules. The hydroxyl group and non-polar alkyl moiety in the molecular structure of ethanol also enable this solvent to dissolve both ionic compounds and non-polar substances, while n-hexane is commonly used in the food industry for the extraction of oils from various foods or spices [33]. Cyclohexane is able to dissolve a wide range of organic compounds. Reverse micelles extraction [34] is able to selectively solubilize polar compounds via the internal water cores of nano-scale aggregates and subsequently transfer the extracted material to the aqueous phase. The exchange of materials across the interface between the two phases is blocked by a layer of these aggregates to produce a separation effect, as shown in Figure 2. As an example, the surfactant dioctyl sulfosuccinate (AOT) has a solubilization effect (Increased solubility) based on the cleavage of hydrogen bonds formed by amide groups and is capable of extracting various analytes or improving extraction efficiency over a wide range of polarity [35].

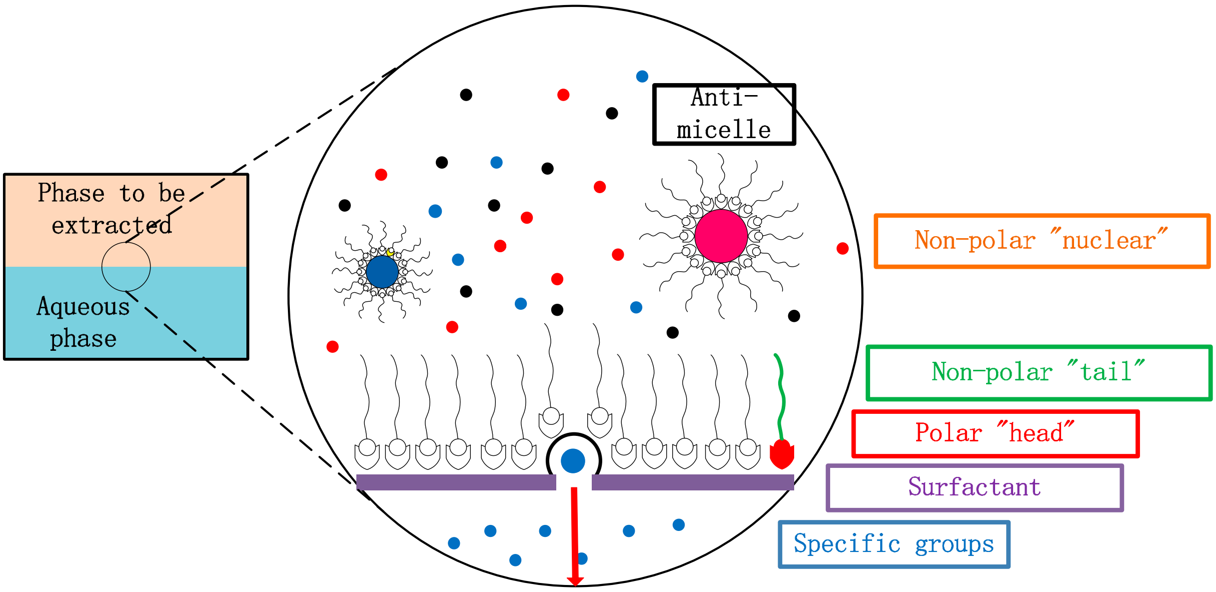

Figure 2. The reverse micelle extraction process. (Figure source: Author's own work).

The present work examined the extraction of coal by n-hexane, cyclohexane (CYH), ethanol (AE), methanol (MT), and a surfactant (AOT), either alone or combined.

2.2. Extraction Procedures

Different types of coal will exhibit variations in pore structure, chemical composition, and functional groups, and long flame coal is more readily extracted compared with lignite, which has a high degree of metamorphism. Long flame coal accounts for the majority of China's raw coal production. Therefore, in this study, raw long flame coal from the Caojiatan mine in northern Shaanxi, China, was employed as a model material (the location of Caojiatan Mine is shown in Figure 3). Fresh coal samples were collected from the working face of the mining area and then sealed and transferred to the laboratory. After unpacking, the outer oxide layer of the raw coal was removed and the coal was pulverized [36]. Both an industrial analysis and elemental analysis of three batches of coal were performed according to the GB/T 212-2008 standard, with the results presented in Table 2.

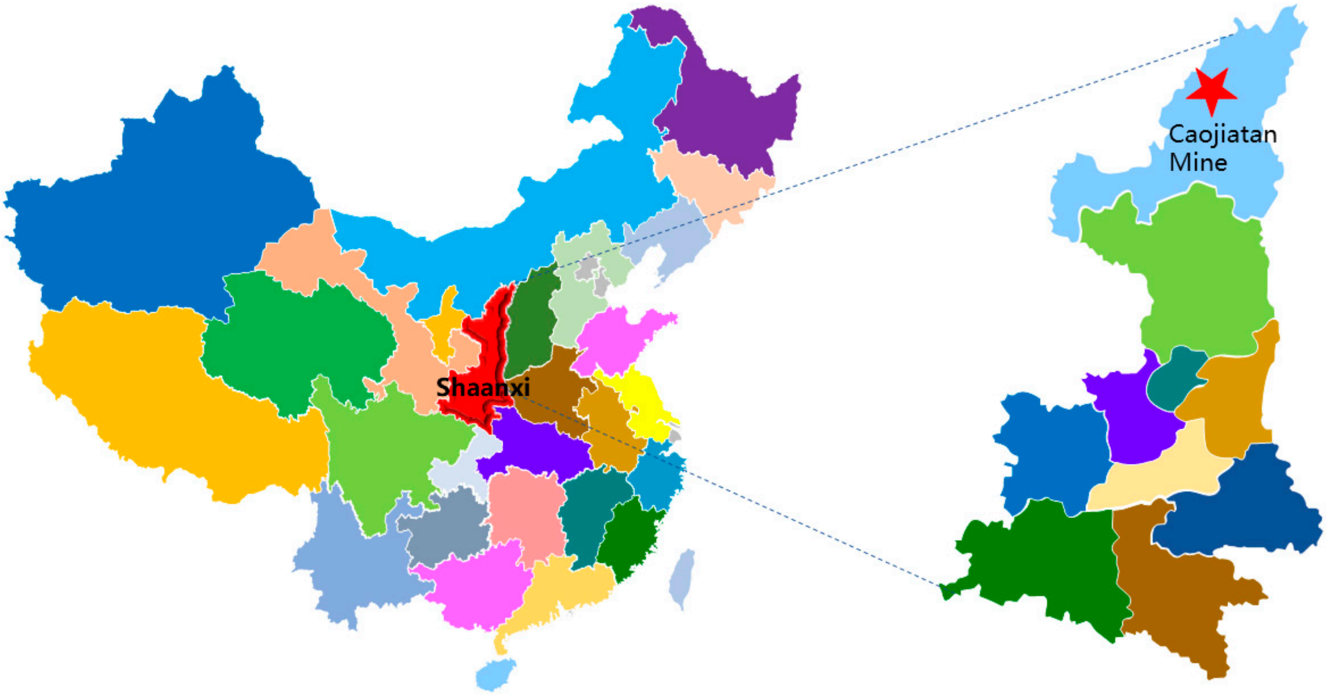

Figure 3. The location of Caojiatan Mine.

Table 2. The results of industrial analysis and elemental analysis of coal samples.

Caojiatan (CJT) Raw Coal Sample	**Proximate Analysis/%**				**Elemental Analysis/%**			
	Moisture Content M_{ad}	**Ash Content** A_d	**Volatile Matter Content** V_d	**Fixed Carbon Content** FC_{ad}	**C**	**H**	**N**	**O**
CJT1	4.72	3.65	35.63	57.85	75.93	4.987	1.135	17.948
CJT2	4.66	3.62	36.17	57.41	75.62	4.966	1.122	18.292
CJT3	4.70	3.57	36.40	57.21	75.91	4.900	1.268	17.922
average value	4.69	3.61	36.06	57.49	75.82	4.951	1.175	18.054

The pulverized coal samples were subsequently screened to obtain specimens with 0–0.12, 0.12–0.15, 0.15–0.18, 0.18–0.25, and 0.25–0.6 mm particle sizes, each with a mass of 200 g. The coal samples in each group were then sealed. A total of 10 groups of extraction solvents (each with a volume of 5 L) were prepared, each containing 20% solute (meaning that 1 kg of coal was added to the 5 L solvent). Each 1 kg coal sample was transferred to a wide-mouth flask along with the solvent, followed by thorough stirring. The flask was subsequently stoppered and allowed to sit under dark conditions for 4 h. Following this static extraction, the coal was collected and dried at 60 °C under a pressure of 0.9 MPa. After drying, the extracted coal was characterized. A small amount of the dry extracted coal sample was removed, weighed, and ground to a particle size of 100–180 mesh then transferred to a sealed tank to be tested. The specific process is shown in Figure 4.

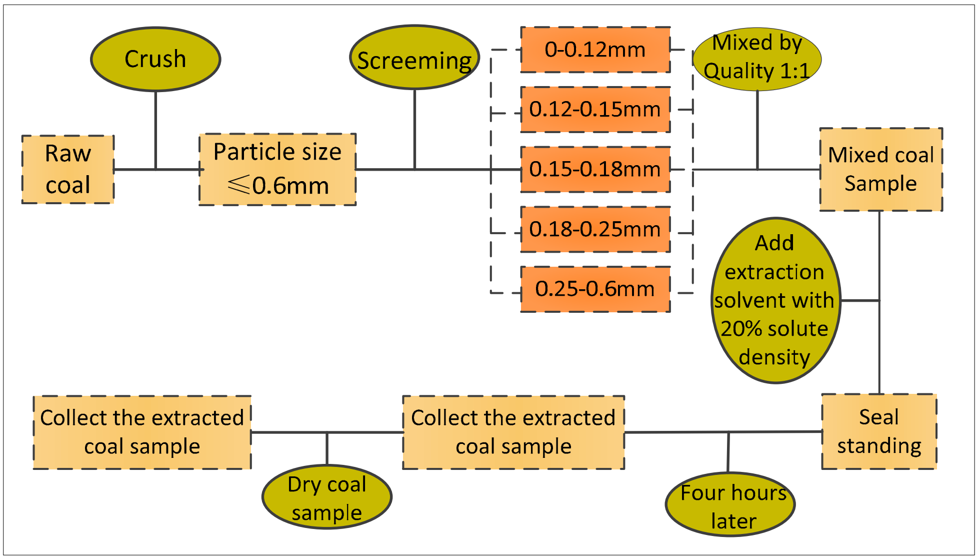

Figure 4. Flow chart summarizing the experimental procedure.

2.3. Extraction Validation

To ensure that the coal samples had been extracted effectively, the extent of extraction was calculated for each specimen based on the mass before and after extraction. The relevant equation is

$$W_i = \frac{(1 - M_{ad}) \times M_1 - M_2}{(1 - M_{ad} - A_d) \times M_1} \times 100\% \tag{1}$$

where W_i is the extent of extraction (%), M_{ad} is the moisture content, A_d is the ash content, M_1 is the mass of the raw coal (g), and M_2 is the mass of the extracted coal sample (g). Single solvent extractions and extractions with synergistic mixtures of solvents (compared to a single solvent) were performed along with a water extraction as a control (decrease error).

2.4. Quantitative Analysis of Functional Groups

FTIR spectra were acquired to quantitatively determine the extent to which various functional groups were extracted, using a Vertex 70V spectrometer with each coal specimen first processed into a KBr pellet. The peak fitting function of the Origin software package was used to process the spectra acquired from each extracted coal sample.

3. Extraction Effectiveness

3.1. Extraction Results

Table 3 summarizes the extraction efficiencies associated with the various solvents.

Table 3. Extraction efficiencies of each solvent.

Test Group	Quality of Raw Coal/g	Quality of the Extracted Coal Sample/g	Extraction Rate/%
MT	1045	953	4.457
CYH	1038	966	2.359
N-Hexane	1022	951	2.449
CYH + AOT + AE	1036	1077	−9.430
AE	1035	960	2.749
AOT	1018	1115	−15.505

It is evident that the AOT provided a negative extraction rate while the extraction efficiencies of the other solvents decreased in the order of MT > AE > n-hexane > CYH. The majority of these common solvents had a limited extraction effect considering the large quantity of coal that was extracted in each trial. Therefore, it is possible that not all functional group structures in the coal samples were completely extracted and lower efficiencies were obtained compared with those obtainable from smaller samples.

The dried specimen following extraction with the AOT contained a white crystalline material mixed among the extracted coal. It is thought that the AOT filled the internal pores of the coal and so was not completely removed, resulting in an apparent increase in mass and the negative extraction value. The present data also indicate that the extraction effects of solvent mixtures were superior to those of single solvents.

3.2. Analysis of Infrared Spectra

As noted, coal molecules are primarily made of macromolecular structures comprising crosslinked chains of aromatic rings. These aromatic backbones also contain side chains and functional groups and are connected via hydrogen bonds and van der Waals forces [37]. In the present work, FTIR spectroscopy was employed to ascertain which functional groups were present in the various specimens. Spectra were acquired from the raw coal samples and six groups of extracted coal using the KBr pellet method. After applying baseline correction and smoothing the spectra the data were compared, as shown in Figure 5.

From Figure 5a, it is apparent that the spectra of the extracted coal samples from the various groups were quite similar to that of the coal immersed in water as a control, with some differences in intensity at certain wavelengths. These spectra exhibit peaks related to C-H bonds at 819 and 876 cm^{-1}, C-O bonds at 1045 and 1084 cm^{-1}, -CH$_3$ groups at 1370 cm^{-1}, C=C bonds between 1447 and 1617 cm^{-1}, -COOH groups at 2338 and 2361 cm^{-1}, -CH$_2$ groups at 2925 cm^{-1}, -CH$_3$ groups at 2968 cm^{-1}, -CH groups at 3060 cm^{-1}, and -OH groups at 3385 cm^{-1}. These spectra indicate that coal molecules containing these groups were readily extracted [38,39]. The spectrum obtained from the raw coal is presented in Figure 5b and the functional groups identified in these materials are summarized in Table 4.

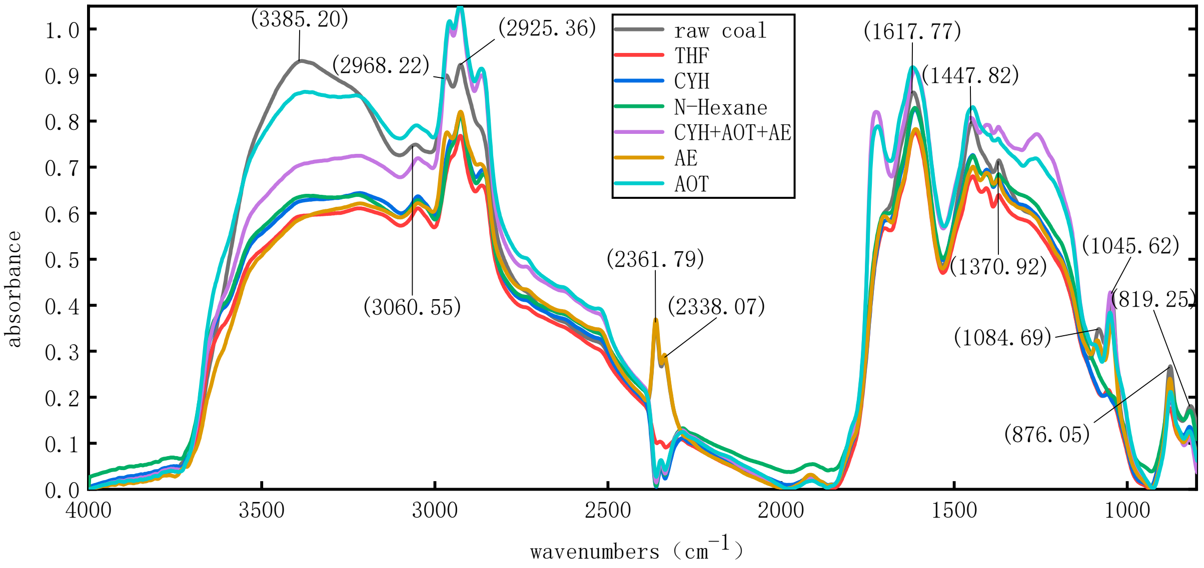

(**a**)

Figure 5. *Cont.*

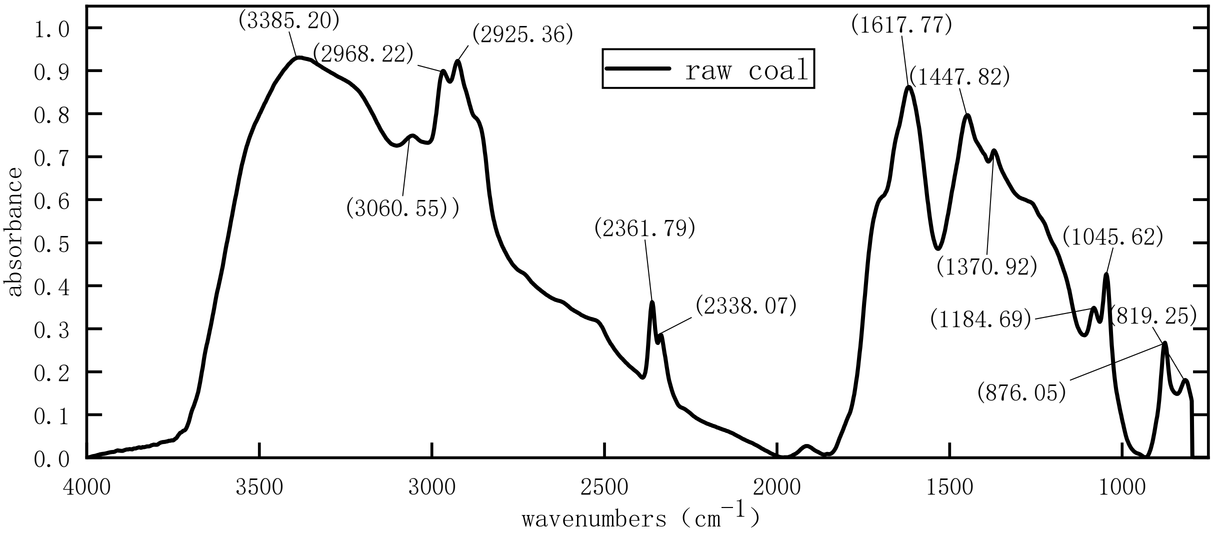

(**b**)

Figure 5. FTIR spectra acquired from (**a**) various extracted coal specimens and (**b**) raw coal.

Table 4. Infrared absorption peaks generated by the raw coal and associated functional groups.

Spectral Peak Number	Peak Position/cm^{-1}	Absorption Peak Band/cm^{-1}	Spectrum Peaks Belonging	The Group Type
1	819	798–840	C-H external bending vibration of ectopic substituted benzene	substituted benzene
2	876	840–931	Substituted benzene C-H out-of-plane bending vibration	substituted benzene
3	1045	931–1064	Saturated fat ether C-O-C symmetric stretching	C-O
4	1084	1064–1108	C-O stretching vibration	C-O
5	1370	1311–1388	-CH_3 symmetric variable Angle vibration	-CH_3
6	1447	1388–1533	C=C frame stretching vibration in aromatic ring/thick ring	C=C
7	1617	1533–1847		C=C
8	2338	2300–2344	-OH stretching vibration in -COOH	-COOH
9	2361	2344–2389		-COOH
10	2925	2883–2946	Methylene C-H stretching vibration	-CH_2
11	2968	2946–3012	Antisymmetric stretching vibration of methyl group	-CH_3
12	3060	3012–3100	Aromatics C-H stretching vibration	-CH
13	3385	3100–3737	-OH in phenols, alcohols, carboxylic acids	-OH

These spectra provide evidence for several peaks related to aromatic structures. Specifically, these peaks comprised the C-H bending vibration of substituted benzene at 819 cm^{-1}, C-H out-of-plane bending vibration of substituted benzene at 876 cm^{-1}, C=C stretching vibrations at 1447 and 1617 cm^{-1}, and C-H stretching vibration at 3060 cm^{-1}. The peaks related to alkyl groups were the -CH_3 symmetric stretching vibration at 1370 cm^{-1}, -CH_2- stretching vibration at 2925 cm^{-1}, and -CH_3 antisymmetric stretching vibration at 2968 cm^{-1}. The main absorption peaks related to oxygen-containing functional groups were attributed to the symmetric expansion of C-O-C in saturated ethers at 1045 cm^{-1}, the C-O stretching vibration at 1084 cm^{-1}, the -OH stretching vibrations of -COOH groups at 2338, and 2361 cm^{-1}, together with an -OH peak at 3385 cm^{-1}. The peak observed at approximately 2400 cm^{-1} was determined to result from CO_2 gas and so can be ignored. It should be noted that only qualitative assessments were possible based on these spectra because of the possibility of overlapping peaks and other issues, and so additional analysis was required.

3.3. Infrared Data Processing

To accurately assess the functional groups in each specimen and evaluate the extraction effects of the solvents, seven groups of spectra were processed by peak fitting to allow quantitative analysis. This peak fitting was performed using the Origin software Peak Fit module with Gaussian fitting and manual selection of peaks. The first derivative of each spectrum was calculated and Savitzky–Golay smoothing was applied, after which suitable functions were obtained for the relevant fitting parameters and sub-peak fitting was performed. Figure 6 presents an example of this process using the spectra obtained from the raw coal. The resulting peak fitting data are summarized in Table 5. The fitting results for the other six groups of FTIR data are shown in Figure 7.

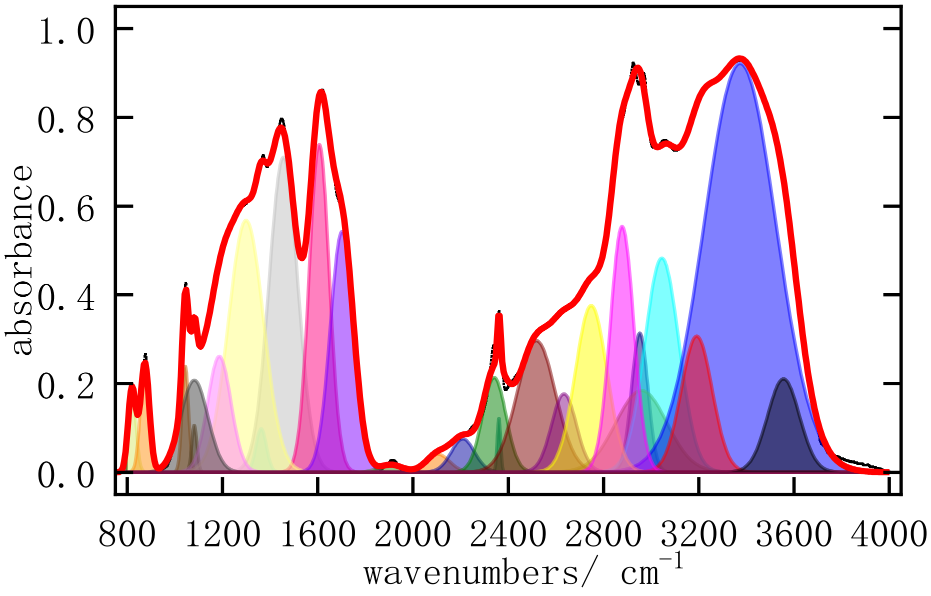

Figure 6. Peak fitting results for the raw coal FTIR spectrum.

Table 5. Peak fitting results for the raw coal FTIR spectrum.

Type	The Average Center	Absorption Peak Attribution	Peak Area
aromatic hydrocarbon	819.8679	substituted benzene	7.73811
	874.0013	substituted benzene	11.41824
	1456.101	C=C	106.9726
	1606.582	C=C	78.49535
	1906.579	C-H	2.10692
	3045.912	aromatic hydrocarbon	86.86852
aliphatic hydrocarbon	1362.781	$-CH_3$	7.33262
	2878.893	$-CH_2$	72.19418
	2953.148	$-CH_3$	35.99535
	2970.776	$-CH_3$	54.26141

Table 5. *Cont.*

Type	The Average Center	Absorption Peak Attribution	Peak Area
oxygen-containing functional group	1043.967	C-O	8.10314
	1080.765	C-O	2.86622
	1083.765	C-O	29.71096
	1186.923	C-O	32.11245
	1299.023	C-O	104.4787
	1702.144	C=O	66.69472
	2104.148	-COOH	4.98769
	2210.091	-COOH	9.21649
	2341.694	-COOH	26.25363
	2361.334	-COOH	2.15573
	2518.659	-COOH	59.63693
	2634.681	-COOH	23.09355
	2749.189	-COOH	62.38078
	3192.25	-OH	50.10662
	3374.61	-OH	349.8566
	3557.065	-OH	35.27509

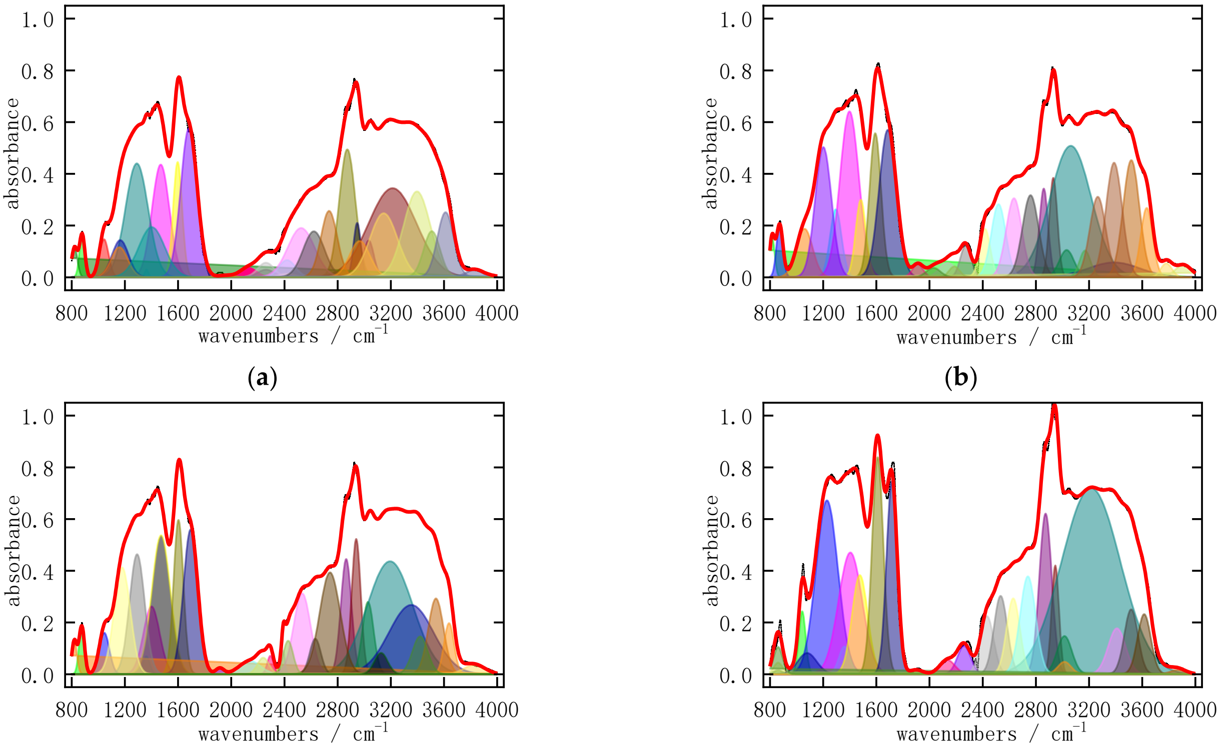

(**a**) (**b**)

(**c**) (**d**)

Figure 7. *Cont.*

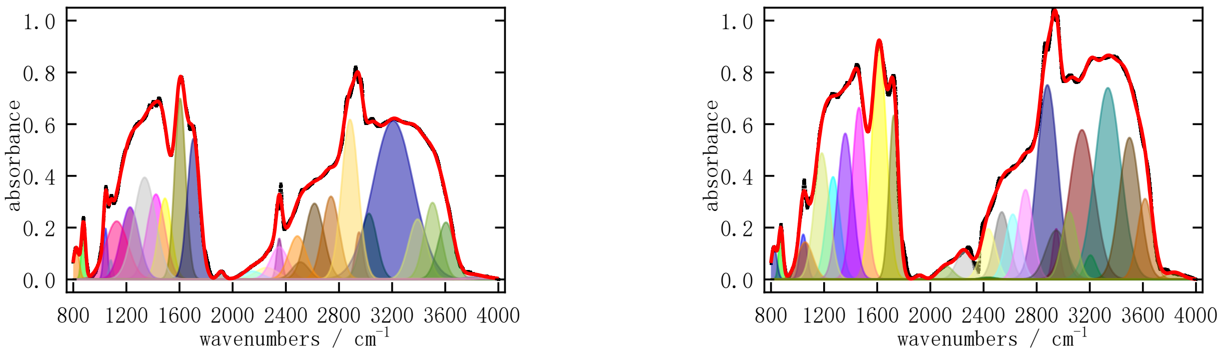

(**e**) (**f**)

Figure 7. Peak fitting results for FTIR spectra acquired from coal samples extracted using (**a**) MT, (**b**) CYH, (**c**) n-hexane, (**d**) CYH + AOT + AE, (**e**) AE and (**f**) AOT.

This peak fitting indicated that several of the original peaks represented two or more overlapping peaks. Therefore, this analytical process was used to assess the functional groups in the coal specimens.

The area of each fitted peak was calculated and the peaks were assigned to oxygen-containing, aromatic, or alkyl structures.

3.4. Quantitative Analysis of Functional Groups

The data in Figures 5–7 allow an assessment of the functional groups in the various extracted coal samples. The results of this assessment are provided in Figure 8.

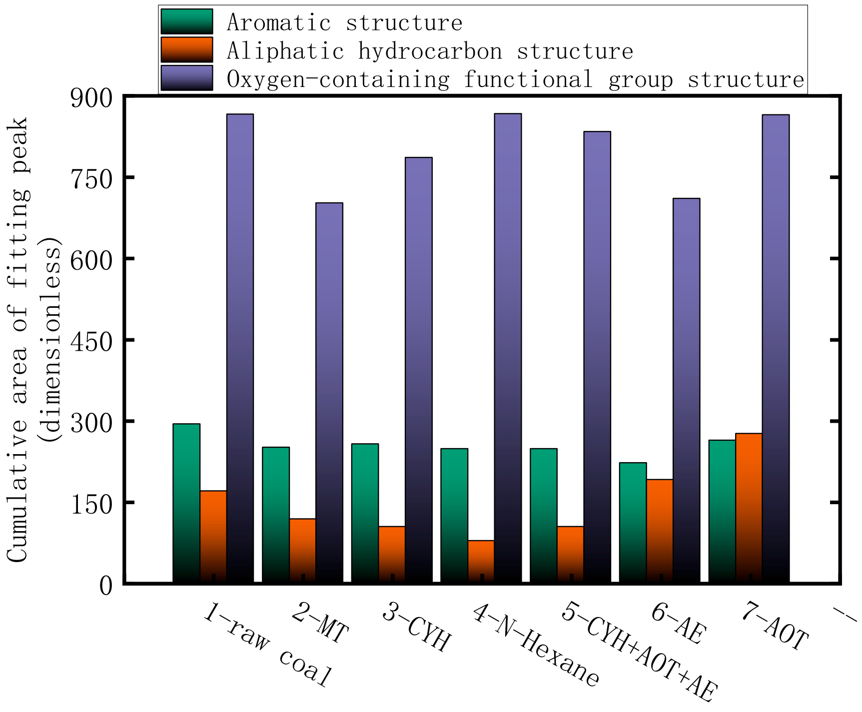

Figure 8. Total areas of FTIR peaks related to group structures in extracted coal samples.

The extent of extraction was determined from the cumulative FTIR peak areas obtained from each extracted coal sample. These cumulative areas were found to decrease in the order of AOT (cumulative area of the peak: 1403) > YM (1330) > n-hexane (1191) > CYH + AOT + AE (1184) > CYH (1145) > AE (1121) > MT (1069) (the later the order, the better the extraction effect). Thus, it was confirmed that all the solvents exhibited relatively effective extraction of the coal. Figure 8 demonstrates that each solvent effectively extracted aromatic structures, although the extraction efficiency decreased in the order of YM > AOT > CYH > MT > n-hexane > CYH + AOT + AE > AE. The best-performing solvents for aromatic groups were therefore n-hexane, CYH + AOT + AE and AE. All solvents showed a good extraction effect for C-H bonds based on the peak at 1920 ± 10 cm^{-1}. The relative proportion of aromatic C=C-H bonds in each of the extracted coal samples was lower than that in the raw coal sample. The material extracted using MT showed the lowest C=C bond content (close to 84% of that in the raw coal). Compared with the other types of functional groups, C=C bonds were found to be more stable and more difficult to degrade during the extraction process.

Figure 8 shows that the various solvents effectively extracted aliphatic structures and this effect decreased in the order of AOT > AE > YM > MT > CYH > CYH + AOT + AE > n-hexane. Thus, the best solvents for this purpose were n-hexane, CYH and CYH + AOT + AE. With the exception of the sample extracted using AOT, the total areas of the peaks at 2875 ± 10 cm^{-1} (the methylene C-H stretching vibration) and 2950 ± 15 cm^{-1} (the methyl group antisymmetric stretching vibration) of all the extracted coal samples were lower than those of the raw coal. The $-CH_3$ content of the material extracted with AOT was higher than that in the raw coal. Figure 8 demonstrates that the various solvents were able to effectively extract coal molecules with oxygen-containing structures. This effectiveness decreased in the order of YM > n-hexane > AOT > CYH + AOT + AE > CYH > AE > MT, and CYH, and AE and MT were the optimal solvents in this regard.

The cumulative areas of the peaks related to C-O bonds between 1100 ± 10 and 1300 ± 20 cm^{-1} in the spectra of the extracted coal samples were lower than those obtained from the raw coal. A comparison of the areas of peaks related to hydroxyl structures between 3250 ± 20 and 3850 ± 5 cm^{-1} indicated that, although the peak area of the CYH + AOT + AE sample was lower than that of the raw coal, the extraction effect of this combination was far lower than those obtained using solely CYH or AE. The peak area of the AOT specimen was closer to that of the raw coal. The area of the peak related to methyl structures obtained from the coal extracted with AOT was approximately 160.49% that of the raw coal sample. Based on the single-phase fluidity of the reverse micelle layer formed by the AOT, it is evident that this surfactant effectively extracted methyl group structures while excluding structures containing -CO and -COOH groups.

4. Conclusions

Methanol, cyclohexane, n-hexane, ethanol, and AOT were used to extract long-flame coal from the Caojiatan Coal Mine. The extraction rate was found to decrease in the order of MT (4.457%) > AE (2.749%) > n-hexane (2.449%) > CYH (2.359%). The cumulative FTIR peak areas obtained from the various trials decreased in the order of AOT (with a value of 1403) > YM (1330) > n-hexane (1191) > CYH + AOT + AE (1184) > CYH (1145) > AE (1121) > MT (1069). The optimal solvents for the extraction of aromatic structures were determined to be n-hexane, CYH + AOT + AE and AE, while those for aliphatic structures were n-hexane, CYH and CYH + AOT + AE. Finally, CYH, AE, and MT showed the most efficient extraction of oxygen-containing structures.

Author Contributions: J.G.: Conceptualization, Supervision, Formal analysis. Y.Q.: Writing (original draft), Formal analysis. H.W.: Methodology, Investigation. X.Z.: Methodology, Investigation. G.C.: Supervision, Formal analysis. Y.J.: Conceptualization, Supervision. All authors have read and agreed to the published version of the manuscript.

Funding: This research was funded by [National Natural Science Foundation of China] grant number [52004209 and 52174198 and 52174197]; Shaanxi Province Qin Chuangyuan “scientist + engineer” innovation team. Mine Fire Intelligent Monitoring, Early Warning and Prevention (2022KXJ-166).

Institutional Review Board Statement: Not applicable.

Informed Consent Statement: Not applicable.

Data Availability Statement: Not applicable.

Conflicts of Interest: The authors declare no conflict of interest.

References

1. Wang, L.C.; Liang, Y.T.; Luo, H.Z. Research progress and prospect of mine thermal dynamic disaster theory in China. *Coal Sci. Technol.* **2018**, *46*, 1–9.
2. Guo, J.; Liu, H.; Jin, Y.; Cai, G.; Liu, Y.; Yang, P. Review of underground coal spontaneous combustion hidden fire detection methods and new technology prospects. *Chin. J. Saf. Sci.* **2022**, *32*, 111–119.
3. Guo, J.; Cai, G.B.; Jin, Y.; Zheng, X. Research progress and trend of coal spontaneous combustion fire prevention technology. *Saf. Coal Mines* **2020**, *51*, 180–184.
4. Zheng, X.Z.; Jia, Y.X.; Guo, J.; Wen, H.; Wang, B. Research status and prospect of coal field fire monitoring technology. *Ind. Mine Autom.* **2019**, *45*, 6–10+61.
5. Wang, D.M.; Shao, Z.L.; Zhu, Y.F. Some scientific problems in coal mine thermal power disaster. *J. China Coal Soc.* **2021**, *46*, 57–64.
6. Tan, B.; Zhu, H.Q.; Wang, H.Y. Structure and key technologies of mine fire intelligent prevention and control. *Saf. Secur.* **2022**, *43*, 1–7+9+89.
7. Li, X.X.; Ma, Y.L.; Wang, D.; Shi, C.Z.; Li, J.; Wang, J.L.; Wang, W.M.; Zhang, S.J.; Zhao, M. Study on chemical constituents of ETOAC extract from corn whisker. *J. Qiqihar Univ. (Nat. Sci. Ed.)* **2020**, *36*, 54–56.
8. Wang, S.; Tao, D.Y.; Meiheriguli, A.; Liu, Q.; Jiang, X.M. Mechanism of antifungal effect of n-butanol extract from Paniculata saliculata on Staphylococcus aureus. *Prog. Vet. Med.* **2019**, *40*, 44–47.
9. Hu, J.P.; Peng, Y.; Liu, F.; Zhang, M.; Peng, C.; Li, B. Screening of antioxidant and antibacterial substances from hawthorn kernel and analysis of chemical constituents by UPLC-Q-TOF/MS. *Food Sci. Technol.* **2020**, *45*, 334–340.
10. Wang, X. Application of supercritical extraction technology in the extraction of anti-aging components from Dandelion. *Chem. Ind. Times* **2022**, *36*, 14–16+39.
11. Deng, J.; Li, Y.Q.; Zhang, Y.T.; Yang, C.; Zhang, J.; Shi, Q. Effect of hydroxyl (-OH) on oxidation characteristics of side chain active groups of coal spontaneous combustion. *J. China Coal Soc.* **2020**, *45*, 232–240.
12. Wang, J.R.; Jin, Z.X.; Deng, C.B. *Quantum Chemistry Theory of Coal Spontaneous Combustion*; Science Press: Beijing, China, 2007; pp. 195–207.
13. Deng, C.B. Study on Spontaneous Combustion Mechanism and Spontaneous Combustion Risk Index of Coal. Ph.D. Thesis, Liaoning Technical University, Fuxin, China, 2006; pp. 12–35.
14. Li, K.J.; Rita, K.; Zhang, J.L.; Barati, M.; Liu, Z.; Xu, T.; Yang, T.; Sahajwalla, V. Comprehensive investigation of various structural features of bituminous coals using advanced analytical techniques. *Energy Fuels* **2015**, *29*, 7187–7189. [CrossRef]
15. Ndaji, F.E.; Butterfield, I.M.; Mark, T.K. Changes in the macromolecular structure of coals with pyrolysis temperature. *Fuel* **1997**, *76*, 169–177. [CrossRef]
16. Zhang, Y.T.; Yang, C.P.; Li, Y.Q.; Huang, Y.; Zhang, J.; Zhang, Y.; Li, Q. Ultrasonic extraction and oxidation characteristics of functional groups during coal spontaneous combustion. *Fuel* **2019**, *242*, 288–294. [CrossRef]
17. Ma, Y.Y.; Ma, F.Y.; Mo, W.L.; Wang, Q. Five-stage sequential extraction of Hefeng coal and direct liquefaction performance of the extraction residue. *Fuel* **2020**, *266*, 10. [CrossRef]
18. Jovanovicalinovska, R.; Kuzmanova, S.; Winkelhausen, E. Application of ultrasound for enhanced extraction of prebiotic oligosaccharides from selected fruits and vegetable. *Ultrason. Sonochem.* **2015**, *22*, 446–453. [CrossRef]
19. Deng, J.; Chen, W.L.; Xiao, Y.; Lu, H.; Wang, H. Experimental study on influence of imidazolium-based ionic liquids on thermo-physical parameters of coal. *J. Xi'an Univ. Sci. Technol.* **2018**, *38*, 523–529.
20. Gorden, J.; Zeiner, T.; Sadowski, G.; Brandenbusch, C. Recovery of cis, cis-muconic acid from organic phase after reactive extraction. *Sep. Purif. Technol.* **2016**, *169*, 1–8. [CrossRef]
21. Marek, S.; Jerzy, S.; Marek, K. Extraction of brown coals with alcohols under supercritical conditions. *J. Energy Inst.* **2020**, *939*, 1933–1998.
22. Liu, C.H. Thermal reaction model construction and oxidation process research of Jurassic coal. Master's Thesis, Xi'an University of Science and Technology, Xi'an, China, 2021.
23. Bai, Z.J. Microscopical characteristics of ionic liquid inhibiting low temperature oxidation of lignite. Master's Thesis, Xi'an University of Science and Technology, Xi'an, China, 2018.
24. Zhang, Y.N.; Liu, C.H.; Shu, P.; Hou, Y.; Yang, J.; Li, L. Study on active group and thermal effect of low temperature oxidation of weak viscose coal. *J. Saf. Sci. Technol.* **2021**, *17*, 98–104.
25. Fan, X.; Xu, H. Research progress of mass spectrometry method in coal molecular structure analysis. *Clean Coal Technol.* **2022**, *28*, 23–30.
26. Niu, Z.Y.; Liu, G.J.; Hao, Y.; Zhou, C.; Wu, D.; Yousaf, B.; Wang, C. Effect of pyridine extraction on the pyrolysis of a perhydrous coal based on in-situ FTIR analysis. *J. Energy Inst.* **2019**, *92*, 428–437. [CrossRef]
27. Hao, Z.C.; Zhang, X.D.; Yang, Y.Q.; Sun, F.Y. Chemical composition and kinetic mechanism of tetrahydrofuran extracts from different coal grades. *J. China Coal Soc.* **2018**, *43*, 2904–2910.
28. Xiao, Y.; Lv, H.F.; Ren, S.J.; Deng, J.; Wang, C. Study on the characteristics of imidazole ionic liquids in inhibiting coal spontaneous combustion. *J. China Univ. Min. Technol.* **2019**, *48*, 175–181.

29. Rahman, M.; Samanta, A.; Gupta, R. Production and characterization of ash-free coal from low-rank Canadian coal by solvent extraction. *Fuel Process. Technol.* **2013**, *115*, 88–98. [CrossRef]
30. Alcalde, R.; Garcia, G.; Atilhan, M.; Aparicio, S. Systematic study on the viscosity of ionic liquids: Measurement and prediction. *Ind. Eng. Chem. Res.* **2015**, *54*, 10918–10924. [CrossRef]
31. Zhang, Q.; Chen, F.S. Effect of reverse micellar extraction on structure and properties of soybean protein isolate. *Food Sci.* **2019**, *40*, 108–113.
32. Yang, W.Q.; Mao, K.M.; Mo, W.L.; Ma, F.Y.; Wei, X.Y.; Fan, X.; Ren, T.Z. Analysis of methanolysis mechanism of extraction residue of Zhumaohu lignite based on reaction path of model compounds. *J. Fuel Chem. Technol.* **2022**, *50*, 396–407. [CrossRef]
33. Zhang, H.L.; Wu, N.Y.; Qiao, X.X.; Huo, R.; Gao, W.; Zhao, X.J. Study on crystallization thermodynamics of lycopene crystal in hexane-acetone mixture. *China Food Addit.* **2021**, *32*, 135–140.
34. Zhang, Q.; Chen, F.S.; Sun, Q. Study on the relationship between microstructure of reverse micelles and pre-extraction rate. *Food Res. Dev.* **2018**, *39*, 4–10.
35. Costi, E.M.; Sicilia, M.D.; Rubio, S. Multiresidue analysis of sulfonamides in meat by supramolecular solvent microextraction, liquid chromatography and fluorescence detection and method validation according to the 2002/657/EC decision. *J. Chromatogr. A* **2010**, *1217*, 6250–6257. [CrossRef] [PubMed]
36. *GB 474-2008*; Method for Preparation of Coal Sample. Standardization Administration of China: Beijing, China, 2008.
37. Sun, Z.Y.; Zhang, X.D.; Zhang, S.; Liu, X.; Zhang, S. Mechanism of composition and chemical structure change of THF soluble low molecular compounds during coal evolution. *J. China Coal Soc.* **2021**, *46*, 3962–3973.
38. Weng, S.F. *Fourier Transform Infrared Spectroscopy*; Chemical Industry Press: Beijing, China, 2010; pp. 377–388.
39. Lu, M.M. Experimental Study on Low-Temperature Oxidation Spontaneous Combustion Characteristics of Jurassic Coal and Its Indicator Gas. Master's Thesis, Xi'an University of Science and Technology, Xi'an, China, 2018; pp. 20–22.